2024 IEEE International Conference on Robotics and Automation (ICRA 2024)
May 13-17, 2024. Yokohama, Japan

Design and Modeling of A Compact Serial Variable Stiffness Actuator (SVSA-III) with Linear Stiffness Profile

Shuowen.Yi, Siyu Liu, Junbei. Liao, Zhao. Guo, *member, IEEE*

***Abstract*—Variable stiffness actuator (VSA) can imitate natural muscles in their compliance capbility, which can provide flexible adaptability for robots, improving the safety of robots interacting with the environment or human. This paper presents a new compact serial variable stiffness actuator ((SVSA-III)) with linear stiffness profile based on symmetrical variable lever arm mechanism. The stiffness motor is used to regulate the position of the pivot located on the Archimedean Spiral Relocation Mechanism (ASRM), so that the stiffness of the actuator can be adjusted (softening or hardening). By designing the lever length, the range of stiffness adjustment can change from 0.3Nm/degree to therotical infinity. Moreover, the continuous linear stiffness profile of the actuator can be customized by solving the transcendental equation of the relationship between the actuator stiffness and the rotation angle of the stiffness motor. SVSA-III has the advantages of compact structure, wide-range stiffness regulation, reduced control difficulty, and linear stiffness profile. Two experiments of step response and stiffness tracking have proved the high accuracy and fast response for both theoretical stiffness and position adjustment.**

I. INTRODUCTION

In recent years, there has been a growing focus on improving the coordination and safety of interactions between robots and humans [1-4]. Compliant actuators, which incorporate elastic elements between the actuator and the load, offer significant advantages in this aspect. These actuators allow for elastic deformation when subjected to external forces, effectively absorbing and mitigating impact forces to minimize the impact on the internal structure and control system of the robot [5-8]. This adaptability to environmental changes makes compliant actuators particularly suitable for robots that require interaction with humans or operate in complex environments [9-10].

One specific type of compliant actuator is the Series Elastic Actuator (SEA), where elastic elements are serially connected between the actuator and the load [11-12]. However, SEA utilizes a fixed stiffness spring, which cannot be adjusted in its physical compliance in practical applications, resulting in its low compliance and limited ability to achieve continuous stiffness adjustment. On the other hand, Variable Stiffness Actuators (VSA), similar to SEA, also incorporate elastic elements but include mechanisms to adjust the stiffness of these elements. By modifying the stiffness during operation, VSA can dynamically adapt to environmental and task demands and offer a method to overcome the limitation of SEA with stiffness adjustment [13-15]. This compliance allows for precise control of robot movements while maintaining high efficiency and reducing energy consumption [16-19].

According to the design principle, VSAs can be classified into two types with antagonistic and serial configurations. [20-25]. Antagonistic VSAs are designed based on the principle of mimicking the antagonistic arrangement of human joints. They feature non-linear springs placed on both sides of the mechanism. By adjusting the positions of these springs through the control of dual motors, the stiffness of the actuator can be adjusted. However, their system has limitations of high energy consumption, low integration level, non-linear stiffness of output joints, and complex control. On the other hand, in the series-type VSAs, such as FSJ [26], AwAS-I [27] and AwAS-II [28], two motors independently control the joint position and stiffness. This mechanism offers clear functionality and has a compact structural design. Our team has developed a series of VSAs using a spiral cam mechanism includes SVSA-I [29], and SVSA-II [30-31], which allows for significant stiffness range. However, in our previous design, the secondary motor typically rotates along with the axis of the primary motor, leading to increased energy consumption. Moreover, the rotation of the secondary motor needs additional space and introduces a significant rotational inertia.

Apart from the attainable range of stiffness, efficiency of regulating stiffness, mechanical size and weight, the stiffness profile is another significant performance that should be considered in the design of a VSA [32-34]. Wang [35] proposed a method to guarantee positioning accuracy and collision safety by utilizing a mechanism with a softening stiffness profile. Shao [36] developed a VSA by a cam-leaf spring mechanism with a predefined stiffness profile to increase the stiffness regulation speed. However, these VSAs still have limitations of large size, complex struture and difficult control.

This paper aims to present a novel compact serial variable stiffness actuator ((SVSA-III)) with linear stiffness profile based on our former SVSA design princple. The contributions of this paper include the following:

(1)A novel symmetrical variable lever arm mechanism based on Archimedean Spiral Relocation Mechanism with

* Research supported by the National Key Research and Development Program of China (No. 2023YFE0202100), the National Natural Science Foundation of China (Grant No. 51605339), and the Key Research and Development Program of Hubei Province (Grant NO. 2020BAB133). Corresponding author to (e-mail: guozhao@whu.edu.cn)

S. Yi, S. Liu, J. Liao and Z. Guo are at School of Power and Mechanical Engineering, Wuhan University, Wuhan, 430072, China.

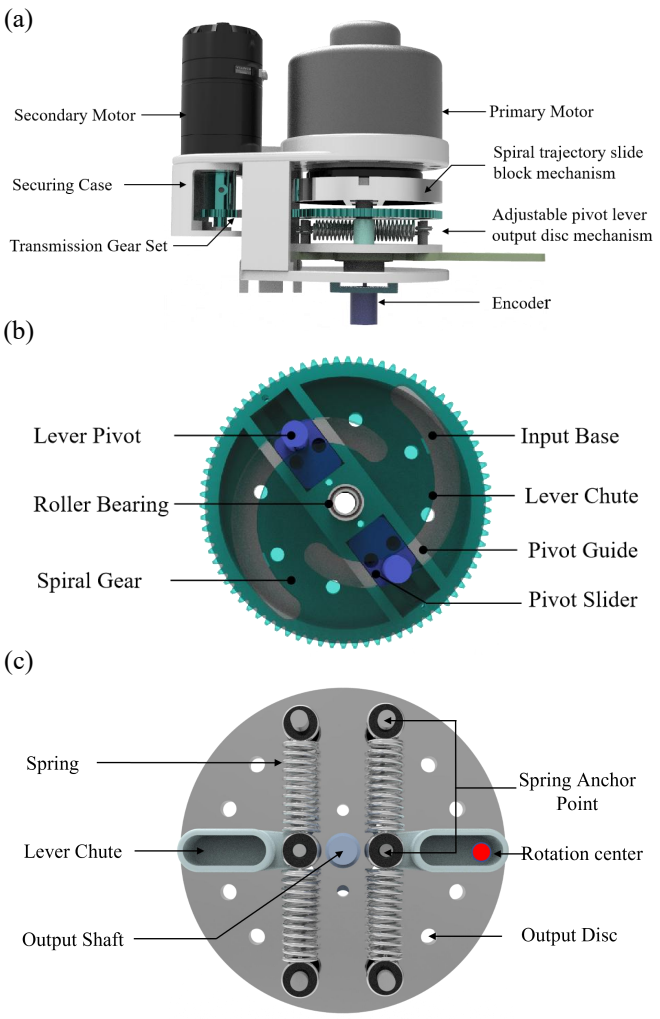

Fig.1. Mechanical design of the SVSA-III: (a) 3D model of the actuator, (b) Archimedean spiral relocation mechanism, (c) variable lever arm mechanism.

movable pivot is proposed. The stiffness is continuously adjusted over a wide range from 0.3Nm/degree to therotical infinity by changing the location of the pivot. Moreover, by solving the transcendental equation of the relationship between the actuator stiffness and the rotation angle of the stiffness motor, the continuous linear stiffness profile of the actuator can be customized, to increase the stiffness adjustment response and reduce control difficulty.

(2) Compared to our former SVSAs, the proposed VSA uses a primary and secondary motor arranged antagonistically, with both motors fixed on the base simultaneously. This setup is more compact and reduces the rotational inertia caused by the rotation of the motor, resulting in a more compact structure.

The remainder of this paper is organized as follows: In section II, the mechanical design and the working principle of the SVSA-III are introduced. In section III, the mathematical modeling is analyzed. The principle of operation and control strategy are introduced in section IV. The prototype implementation and evaluation experiment are presented in section V. Finally, conclusion and future works are discussed in section VI.

II. Mechanical Design of the SVSA-III

A. Mechanical Design

As shown in Fig.1(a), SVSA-III consists of three parts: the drive mechanism, the spiral trajectory slide block mechanism, and the adjustable pivot lever output disc mechanism. The axial position of the spiral trajectory slide block mechanism and the adjustable pivot lever output disc mechanism is achieved by the securing case, gaskets and thrust roller bearings, which make a compact structure and reduce internal friction. Considering the possible slight bending deformation when the spring is compressed, this design intends to use tension springs to eliminate instability due to spring bending. With the output shafts of the primary and secondary motors aligned parallelly, the periodic jamming resistance of the gear may occur, owing to the co-axial accuracy's influence. Thus, the transmission gear set is designed as positive correction displacement arrangement.

Archimedean spiral relocation mechanism: as shown in Fig.1(b), Archimedean spiral gear and input base are separated by thrust roller bearings, which ensures the relative position of the two and reduces energy loss due to axial friction. The spirals are centrally symmetric distribution on the Archimedean spiral gear, adjusting the pivot slider's trajectory through rotation. The range of pivot's motion is constrained by lever chute and pivot guide.

As shown in Fig. 1(c), the variable lever arm mechanism is composed of four springs and two lever chutes. The springs are symmetrically dispersed and respectively anchored at the lever chute ends and spring anchor point on the output disc. One end of the lever chute is fixed to the output disc as the rotational center using deep groove ball bearings, while the other end rotates around the rotational center, causing the spring to stretch or compress.

B. Principle of the SVSA-III

As shown in Fig. 2, there are two operating modes for adjusting the stiffness of SVSA-III. As shown in Fig. 2 (a) and (b), one is to keep the output disc fixed, so that when the secondary motor rotates the spiral gear through the gear transmission, the spiral chute will induce symmetric movement in the slides. This changes the relative position of the slide on the lever chute which can adjust the lever arm, thereby achieving stiffness adjustment. The other one is to keep the input base fixed under load, so that when the lever's pivot revolves around its center of rotation, a quantifiable restorative elastic force is provided by the deformed spring shown in Fig. 2(c). The pivot of the slider, changing the moment arm's length through its traverse in the track of the lever, vary the torque, thus adjusting the softness to be eventually output through the output shaft. Due to the leveraging effect, as the moment arm diminishes i.e., the pivot converges towards the lever's center of rotation, its stiffness multiplies, potentially peaking at an absolute stiffness. On the contrary, the pivot converges towards the spring, its stiffness can realize 0.3Nm/degree.

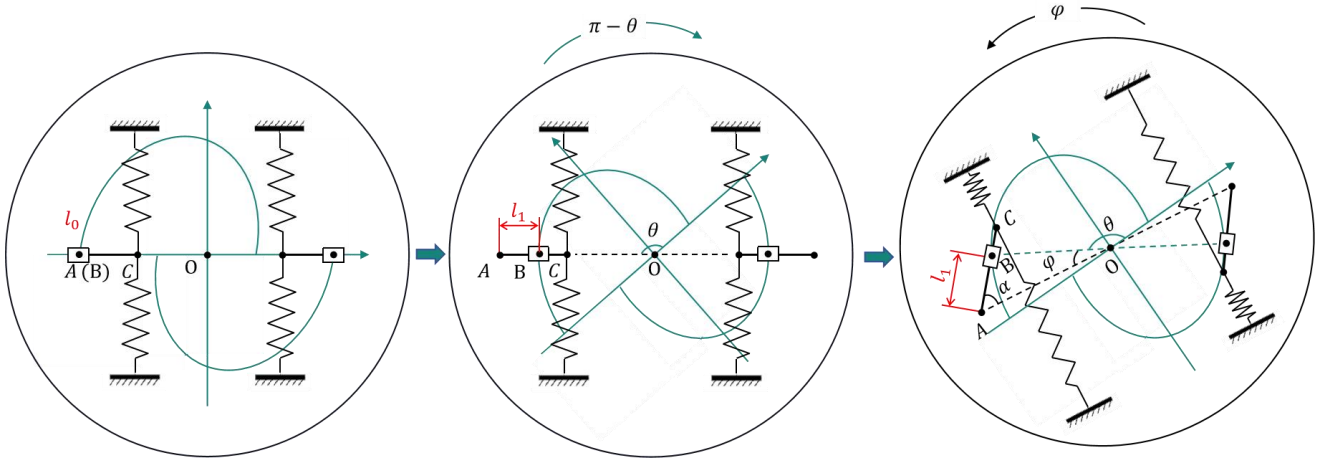

Fig.2. The working principle of the SVSA-III: (a) initial position of the VSM (b) stiffness regulation when output base is fixed (c) stiffness regulation when input base is fixed under load. AC is the lever chute;*l* is the length of the AB; point A is the center of rotation for the lever chute; point B is the lever pivot; point C is the anchor point for the spring; φ is the elastic deflection angle of the actuator output end; θ is the rotation angle of spiral gear; *l* is the lever chute arm.

III. Modeling of the SVSA-III

As shown in Fig. 2, the variable lever arm mechanism can be simplified into the following model. The range of elastic deflection angle at the output end of the actuator in Fig. 3 is generally less than 10 degrees, which can be approximately considered as the spring's length change in the vertical direction, neglecting its inclined deviation.

The equation for the spiral is

$$\rho = e + f\theta \tag{1}$$

e and f respectively represent the initial radius of the spiral and the increase in the radius of the spiral per unit degree, θ is the rotation angle of spiral gear.

The relationship between the angle and position of the lever slider is represented as

$$\begin{cases} a\sin\alpha = \rho\sin\varphi \\ b\sin\alpha = \rho\sin(\alpha+\varphi) \\ a^2 = \rho^2 + b^2 - 2\rho b\cos\varphi \end{cases} \tag{2}$$

Considering the linear deformation of the spring, the static equilibrium equations of the lever can be calculated as

$$\begin{cases} F_\varphi a = F_\alpha l_{AC}\cos\alpha \\ F_\alpha = 2kl_{AC}\sin\alpha \end{cases} \tag{3}$$

Where k is the stiffness of a spring, it is calculated from the linear spring formula, yielding a value of 7500N/m.

The theoretical torque output τ_{des} of the output shaft can be calculated as

$$\tau_{des} = 2F_\varphi\rho\cos(\alpha+\varphi) \tag{4}$$

The stiffness of the output shaft K can be calculated as

$$K = \frac{\tau_{des}}{\varphi} \tag{5}$$

According to equations (1) ~ (5), the output stiffness K, the rotation angle of spiral gear θ , and deflection angle φ expressions can be obtained as

$$\begin{cases} K = \dfrac{4l_{AC}^{\ 2}(e+f\theta)\sin\alpha\cos\alpha\cos(\alpha+\varphi)}{a\varphi} \\ \alpha = \arcsin\dfrac{(e+f\theta)\sin\varphi}{a} \end{cases} \tag{6}$$

The numerical solution for the stiffness relationship is obtained as shown in Fig. 4.

Due to the exponential equations and trigonometric functions forming the relationship between output stiffness K, the rotation angle of spiral gear θ , and deflection angle φ , it results in a transcendental equation which is difficult to solve analytically. The specific relationship equation can be written as

$$\theta(K,\varphi) = A_{n+1}(K)x_{n+1}(\varphi) \tag{7}$$

Where $A_n(K)$ is the coefficient matrix related to the equivalent stiffness K, $x_n(\varphi)$ is the polynomial matrix composed of the deflection angle. n and m represent the degrees of the polynomial fitting. By using polynomial fitting, we can calculate

$$\begin{cases} A_{n+1}(K) = (a_0(K),\cdots,a_n(K)) \\ a_{n+1}(K) = b_{a_{n+1},0}K^0 + \cdots + b_{a_{n+1},\mathrm{m}}K^m \\ x_{n+1}(\varphi) = (\varphi^0,\cdots,\varphi^n)^T \end{cases} \tag{8}$$

According to formulas (7) ~ (8), the final fitting relationship can be expressed as

$$\theta(K,\varphi) = \left(K^0,\cdots,K^m\right)\begin{pmatrix} b_{a_1,0} & \cdots & b_{a_{n+1},0} \\ \vdots & \ddots & \vdots \\ b_{a_1,\mathrm{m}} & \cdots & b_{a_{n+1},\mathrm{m}} \end{pmatrix}\begin{pmatrix} \varphi^0 \\ \vdots \\ \varphi^n \end{pmatrix} \tag{9}$$

IV. Control Design Of The SVSA-III

When SVSA-III is loaded, with the benefit from the variable lever arm mechanism, deflection angle of the output disc φ can be easily measured by an encoder which is connected with the output shaft. Thus, the actual output

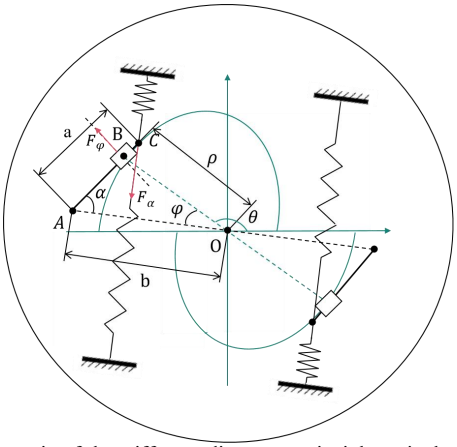

Fig. 3. Schematic of the stiffness adjustment principle. ρ is the position of the slider B relative to the center rotation point O; b is the distance from the lever pivot A to the total rotation point O; a is the distance of slider B relative to the pivot center A; α is the rotation angle of the lever; F_φ is the elastic force received by the slider perpendicular to the direction of the lever; F_α is the spring force provided by the spring.

angle of the VSA q could be calculated from the difference between the position of the primary motor q_{pout} and actual deflection angle

$$q = q_{pout} - \varphi \tag{10}$$

Due to friction and modeling accuracy issues, the actual stiffness of VSA does not match the desired stiffness K_{des}, which means that the output position q and torque τ_{out} do not match the desired position q_{des} and torque τ_{des}. Therefore, as shown in Fig. 6, we designed a controller to improve the accuracy of VSA stiffness output. λ is the gear ratio between the spiral and the secondary motor. τ_{ext} is the external load. The desired position q_{des} and stiffness K_{des} are provided by the trajectory generator. The desired torque τ_{des} can be calculated by Eq. (5) and (6), which can be turned into the desired rotation angle of spiral gear θ_{des}. The actual torque output τ_{out} can be measured by a force sensor. The output angle of the secondary motor is the sum of the output angle of the primary motor and the rotation angle of gear $\lambda\theta_s$,which can be calculated as

$$q_{sout} = q_{pout} + \lambda\theta_s \tag{11}$$

We use Eq. (9) to calculate the desired position of the secondary motor θ_{des} by taking into account the deflection angle and desired stiffness. It will then convert torque to position control with Eq. (5) and (6), thereby the position control of the primary motor.

$$u_q = k_{Pq}e_q + k_{Dq}\dot{e}_q + k_{Fqv}\dot{q}_{des} + k_{Fqa}\ddot{q}_{des} \tag{12}$$

$$u_\theta = k_{P\theta}e_\theta + k_{D\theta}\dot{e}_\theta + k_{F\theta v}\dot{\theta}_{des} + k_{F\theta a}\ddot{\theta}_{des} \tag{13}$$

where u_q and u_θ are the control commands of the primary and secondary control motors, respectively. e_q and e_θ are the input errors for the PD controller where $e_q = q - q_{des}$ and $e_\theta = \theta_{out} - \theta_{des}$. K_{pq} and $K_{p\theta}$ are the proportional gains, K_{Dp} and $K_{D\theta}$ are the derivative control gains. K_{Fqv} and $K_{F\theta v}$ are the feedforward coefficients for velocity compensation, K_{Fqa} and $K_{F\theta a}$ are the coefficients for acceleration compensation.

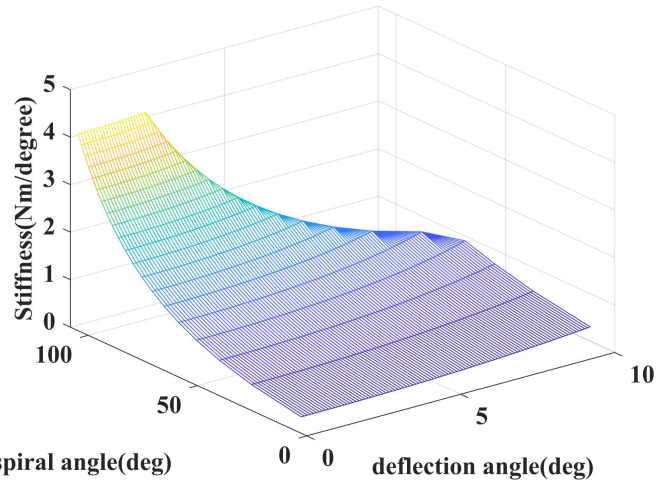

Fig. 4. The relationship between the stiffness, rotational angle of spiral, and torsion angle.

TABLE I
GENERAL SPECIFICATIONS FOR THE SVSA-III.

SVSA-III	Value
Spiral gear teeth number	78
Secondary motor gear teeth number	19
Gear material	45 # steel
Other components materials	6061 alloy
Gear module m (mm)	1
Leverage total length a (mm)	23
Lever pivot radius b (mm)	33
Secondary motor rated output torque (Nm)	3
Primary motor peak output torque (Nm)	23
Actuator diameter (mm)	90
Actuator axial length (mm)	31
Actuator rotation angle (deg)	-120~120
Deflection angle (deg)	-10~10
Spring stiffness coefficient (N/m)	7500
Range of stiffness (Nm/deg)	0.3~∞

V. EXPERIMENTS AND RESULTS

In order to verify the accuracy of the modeling and the mechanical performance of the variable stiffness actuator, step response and stiffness tracking tests were conducted in this section. as shown in Fig. 7, a torque sensor was installed at the output disc of the VSA-III and the output disc was fixed. By setting the stiffness curve of the variable stiffness actuator, the bottom-layer position outputs of the primary motor and the secondary motor were controlled to achieve stiffness changes. The specific parameters of the SVSA-III are shown in Table 1.

Experiments

1) **Step response experiment:** Step response experiment was conducted using three different stiffness values: 1Nm/degree, 1.6Nm/degree, and 2Nm/degree. The primary motor was set to signal of 5 degrees. To maintain constant stiffness, the secondary motor was required to follow the step of the primary motor. The step torque output of the VSA was measured using a force sensor, and the theoretical

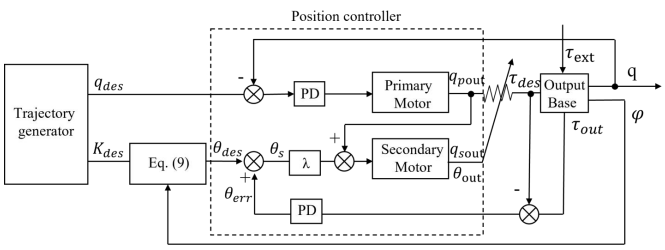

Fig. 6. Controller design for the VSA.

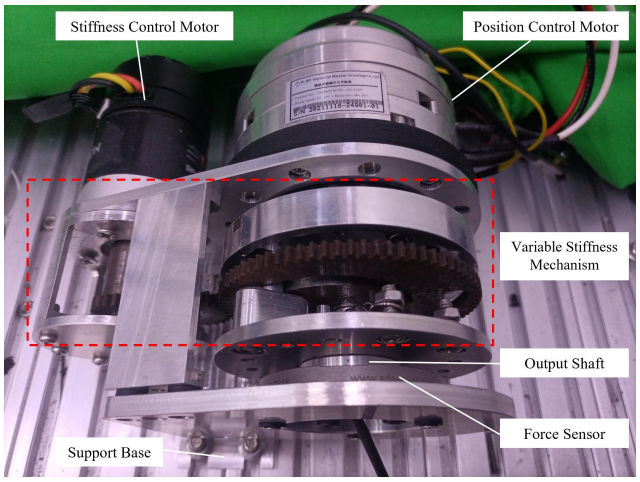

Fig. 7. Prototype of the SVSA-III.

torque values were 5Nm, 8Nm, and 10Nm respectively, as shown in Fig. 8(a), (b), and (c). Experimental data is presented in Figure 8. It can be observed from the figure that the step response time of the VAS was within 0.2s under the three mentioned stiffness conditions, indicating a fast response speed.

The experiment diagram as shown in Fig. 8, representing torque tracking, is transformed into a stiffness profile as shown in Fig. 9. The dashed line represents the desired stiffness at three different levels for the VSA, and the solid line represents the actual torque output by the motor corresponding to the desired stiffness. From Fig. 9, it can be observed that the actual result is close to the theoretical result which means by solving the transcendental equation for constant stiffness, VSA with linear spring properties can be developed. It can also be seen that the VSA exhibits a hysteresis phenomenon, which is a result of the error produced by the stiffness control motor. In future applications, corresponding feedforward compensation should be implemented to eliminate the effects of hysteresis and VSA with nonlinear stiffness profile will be verified.

2) **Stiffness tracking experiment**: In the stiffness tracking experiment, the primary motor was fixed the output angle at 5 degrees. The average input stiffness was 1.0 Nm/degree, with an amplitude of 0.6 Nm/degree, and a sine stiffness curve with a frequency of 0.5 Hz, which can be presented as

$$K = 0.6\sin(0.5\cdot t)+1 \tag{14}$$

The output angle of the secondary motor is determined by

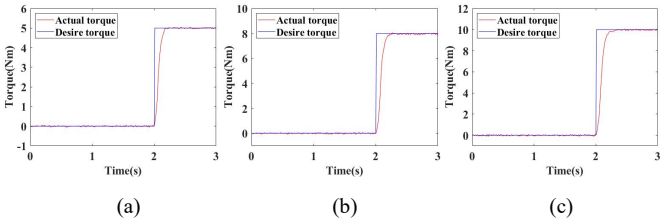

Fig. 8. Step response for torque control.

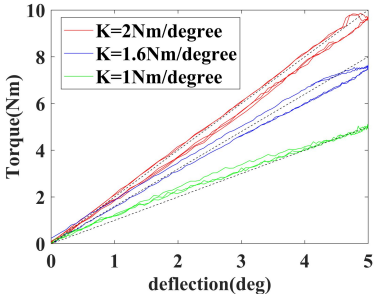

Fig. 9. Results of the VSA with a linear stiffness profile.

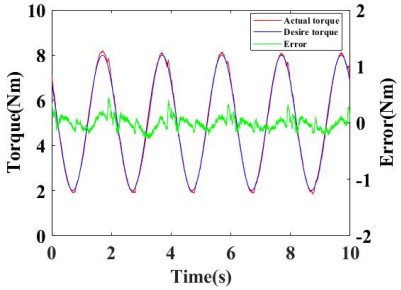

Fig. 10. Stiffness tracking experiment.

equation (9), so the theoretical torque can be calculated as

$$\tau = 3\sin(0.5\cdot t)+5 \tag{15}$$

Experimental data is presented in Fig. 10. The variable stiffness torque exhibits a maximum error of 0.4512 Nm under the conditions of a sinusoidal expected stiffness with an average of 1 Nm/degree, an amplitude of 0.6 Nm/degree, and a fixed output angle of 5 degrees. Furthermore, calculations indicate that the maximum error for stiffness tracking is 0.090 Nm/degree, accounting for 9.0% of the total average stiffness, for an average stiffness with an amplitude of 0.6 Nm/degree.

The results suggest that the VSA is able to accurately track the theoretical stiffness curve. However, there is slight error of the stiffness curve, resulting from the frictions between the spiral gear and the slider. Further structural optimization is considered to minimize the friction impact between these two components.

VI. Conclusion

In this work, a compact serial variable stiffness actuator (SVSA-III) with linear stiffness profile based on the variable lever arm mechanism has been presented. With the benefit from the ASRM, VSA with linear spring properties can be developed by solving the transcendental equation for constant stiffness. Two experiments are investigated to

evaluate the performance of the new actuator to prove the high accuracy and fast response for both theoretical stiffness and position adjustment. Future work will focus on the VSA-III with nonlinear stiffness profile and its application on robotics.

REFERENCES

[1] R. Huang, H. Cheng, J. Qiu and J. Zhang, "Learning physical human–robot interaction with coupled cooperative primitives for a lower exoskeleton", *IEEE Trans. Autom. Sci. Eng.*, vol. 16, no. 4, pp. 1566-1574, Oct. 2019.

[2] Z. Li, B. Huang, Z. Ye, M. Deng and C. Yang, "Physical human–robot interaction of a robotic exoskeleton by admittance control", *IEEE Trans. Ind. Electron.*, vol. 65, no. 12, pp. 9614-9624, Dec. 2018.

[3] Y. Zhu and S. Bai, "Human Compatible Stiffness Modulation of a Novel VSA for Physical Human-Robot Interaction," *IEEE Robotics and Automation Letters,* vol. 8, no. 5, pp. 3023-3030, May 2023.

[4] D. Rodriguez-Cianca et al., "A variable stiffness actuator module with favorable mass distribution for a bio-inspired biped robot", *Front. Neurorobot*., vol. 13, 2019.

[5] Z. Li, S. Bai, O. Madsen, W. Chen and J. Zhang, "Design modeling and testing of a compact variable stiffness mechanism for exoskeletons", *Mech. Mach. Theory*, vol. 151, 2020.

[6] H. Yu, S. Huang, G. Chen, and N. Thakor, "Control design of a novel compliant actuator for rehabilitation robots," *Mechatronics*, vol. 23,no. 8, pp. 1072–1083, Dec. 2013

[7] Y. Pan, Z. Guo, X. Li and H. Yu, "Output-Feedback Adaptive Neural Control of a Compliant Differential SMA Actuator," *IEEE Transactions on Control Systems Technology*, vol. 25, no. 6, pp. 2202-2210, Nov. 2017.

[8] X. Li, Y. Pan, G. Chen, and H. Yu, "Continuous tracking control for a compliant actuator with two-stage stiffness," *IEEE Trans. Autom. Sci.Eng.*, vol. 15, no. 1, pp. 57–66, Jan. 2018.

[9] Y. Ning, Y. Liu, F. Xi, K. Huang and B. Li, "Human-robot interaction control for robot driven by variable stiffness actuator with force self-sensing", *IEEE Access*, vol. 9, pp. 6696-6705, 2021.

[10] V. Grosu, C. Rodriguez-Guerrero, S. Grosu, B. Vanderborght, and D. Lefeber, "Design of smart modular variable stiffness actuators for robotic-assistive devices," *IEEE/ASME Trans. Mechatronics*, vol. 22,no. 4, pp. 1777–1785, Aug. 2017.

[11] E. A. Bolívar Nieto, S. Rezazadeh and R. D. Gregg, "Minimizing Energy Consumption and Peak Power of Series Elastic Actuators: A Convex Optimization Framework for Elastic Element Design," *IEEE/ASME Trans. Mechatronics*, vol. 24, no. 3, pp. 1334-1345, June 2019

[12] H. Yu, S. Huang, G. Chen, Y. Pan and Z. Guo, "Human–robot interaction control of rehabilitation robots with series elastic actuators," *IEEE Trans. Robot.*, vol. 31, no. 5, pp. 1089-1100, Oct. 2015.

[13] S. S. Groothuis, S. Stramigioli and R. Carloni, "Modeling robotic manipulators powered by variable stiffness actuators: A graph-theoretic and port-Hamiltonian formalism," *IEEE Trans. Robot.,* vol. 33, no. 4, pp. 807-818, Aug. 2017.

[14] A. Jafari, N. G. Tsagarakis and D. G. Caldwell, "A novel intrinsically energy efficient actuator with adjustable stiffness (AWAS)", *IEEE/ASME Trans. Mechatronics*, vol. 18, no. 1, pp. 355-365, Feb. 2013.

[15] N. G. Tsagarakis, I. Sardellitti and D. G. Caldwell, "A new variable stiffness actuator (compact-VSA): Design and modelling", *Proc. IEEE/RSJ Int. Conf. Intell. Robots Syst.(IROS)*, pp. 378-383, 2011

[16] S. S. Groothuis, G. Rusticelli, A. Zucchelli, S. Stramigioli and R. Carloni, "The VSAUT-II: A novel rotational variable stiffness actuator", *Proc. IEEE Int. Conf. Robot. Automat.*, pp. 3355-3360, 2012..

[17] S. Wolf and J.-E. Feenders, "Modeling and benchmarking energy efficiency of variable stiffness actuators on the example of the DLRFSJ," in Proc. *IEEE/RSJ Int. Conf. Intell. Robots Syst. (IROS),* Oct. 2016,pp. 529–536.

[18] S. Wolf, O. Eiberger, and G. Hirzinger, "The DLR FSJ: Energy based design of a variable stiffness joint," in Proc. *IEEE Int. Conf. Robot Autom.(ICRA)*, May 2011, pp. 5082–5089.

[19] HQ. Vu, X. Yu, F. Iida, R. Pfeifer, "Improving Energy Efficiency of Hopping Locomotion by Using a Variable Stiffness Actuator," *IEEE/ASME Trans. Mechatronics*, vol: 21, no.1, pp. 472- 486, 2016.

[20] Z. Guo, Y. Pan, L. B. Wee, H. Yu, "Design and control of a novel compliant differential shape memory alloy actuator," *Sensors and Actuators A*, vol. 225, no. 3, pp. 71-80, 2015.

[21] A. Jafari, "Coupling between the Output Force and Stiffness in Different Variable Stiffness Actuators," *Actuators*, vol. 3, no. 3, pp. 270-284, 2014.

[22] R. Mengacci, M. Garabini, G. Grioli, M. G. Catalano and A. Bicchi, "Overcoming the Torque/Stiffness Range Tradeoff in Antagonistic Variable Stiffness Actuators," *IEEE/ASME Trans. Mechatronics*, vol. 26, no. 6, pp. 3186-3197, Dec. 2021.

[23] S. Wolf, G. Grioli, O. Eiberger, W. Friedel, et al., "Variable Stiffness Actuators: Review on Design and Components," *IEEE/ASME Trans. Mechatronics*, vol: 21, no.5, pp. 2418- 2430, 2016

[24] F. Petit, W. Friedl, H. Höppner and M. Grebenstein, "Analysis and Synthesis of the Bidirectional Antagonistic Variable Stiffness Mechanism," *IEEE/ASME Trans. Mechatronics*, vol. 20, no. 2, pp. 684-695, April 2015.

[25] R. Mengacci, M. Keppler, M. Pfanne, A. Bicchi and C. Ott, "Elastic Structure Preserving Control for Compliant Robots Driven by Agonistic-Antagonistic Actuators (ESPaa)," *IEEE Robot. Autom. Lett.*, vol. 6, no. 2, pp. 879-886, April 2021.

[26] S. Wolf, O. Eiberger, and G. Hirzinger, "The DLR FSJ: Energy based design of a variable stiffness joint," *Proc. IEEE Int. Conf. Robot. Autom.*, 2011, pp. 5082-5089.

[27] A. Jafari, N. G. Tsagarakis and D. G. Caldwell, "A Novel Intrinsically Energy Efficient Actuator With Adjustable Stiffness (AwAS)," in *IEEE/ASME Trans. Mechatronics*, vol. 18, no. 1, pp. 355-365, Feb. 2013.

[28] A. Jafari, N. G. Tsagarakis, I. Sardellitti, and D. G. Caldwell, "A new actuator with adjustable stiffness based on a variable ratio lever mechanism," *IEEE/ASME Trans. Mechatronics*, vol. 19, no. 1, pp. 55–63,Feb. 2014.

[29] J. Sun, Y. Zhang, C. Zhang, Z. Guo and X. Xiao, "Mechanical design of a compact Serial Variable Stiffness Actuator (SVSA) based on lever mechanism," *2017 Proc. IEEE Int. Conf. Robot. Automat*., *(ICRA)*, Singapore, 2017.

[30] J. Sun, Z. Guo, Y. Zhang, X. Xiao and J. Tan, "A Novel Design of Serial Variable Stiffness Actuator Based on an Archimedean Spiral Relocation Mechanism," *IEEE/ASME Trans. Mechatronics*, vol. 23, no. 5, pp. 2121-2131, Oct. 2018.

[31] J. Sun, Z. Guo, D. Sun, S. He, and X. Xiao, "Design, modeling and control of a novel compact, energy-efficient, and rotational serial variable stiffness actuator (SVSA-II)," *Mechanism Mach. Theory*, vol. 130, pp. 123 – 136, Dec. 2018.

[32] C. Wang et al., "A lightweight series elastic actuator with variable stiffness: Design, modeling, and evaluation," *IEEE/ASME Trans. Mechatronics*, early access, Mar. 24, 2023,

[33] Z. Song, D. Gao, Y. Zhao, and J. S. Dai, "An improved Bouc–Wen model based on equitorque discretization for a load-dependent nonlinear stiffness actuator," *IEEE Trans. Autom. Sci. Eng*., vol. 18, no. 2, pp. 840–849, Apr. 2021.

[34] X. Hu, Z. Song, and T. Ma, "Novel design method for nonlinear stiffness actuator with user-defined deflection-torque profiles," *Mechanism Mach. Theory*, vol. 146, Apr. 2020, Art. no. 103712

[35] Z. Wang et al., "Design of a novel compliant safe robot joint with multiple working states," *IEEE/ASME Trans. Mechatronics*, vol. 21, no. 2, pp. 1193–1198, Apr. 2016.

[36] Y. Shao, D. Shi, W. Zhang and X. Ding, "Design and Evaluation of Variable Stiffness Actuators with Predefined Stiffness Profiles," *IEEE Trans. Autom. Sci. Eng.,* 2023.